

Non-standard interaction effects on astrophysical neutrino fluxes

Mattias Blennow^{1,*} and Davide Meloni^{2,†}

¹*Max-Planck-Institut für Physik (Werner-Heisenberg-Institut),*

Föhringer Ring 6, 80805 München, Germany

²*Dipartimento di Fisica, Università di Roma Tre and INFN Sez. di Roma Tre,*

via della Vasca Navale 84, 00146 Roma, Italy

(Dated: November 20, 2018)

Abstract

We investigate new physics effects in the production and detection of high energy neutrinos at neutrino telescopes. Analysing the flavor ratios ϕ_μ/ϕ_τ and $\phi_\mu/(\phi_\tau + \phi_e)$, we find that the Standard Model predictions for them can be sensibly altered by new physics effects.

PACS numbers: 14.60.Lm, 14.60.Pq, 95.55.Vj, 95.85.Ry

*blennow@mppmu.mpg.de

†meloni@fis.uniroma3.it

I. INTRODUCTION

Neutrino oscillation physics has definitively entered the era of precision measurements of the fundamental neutrino parameters. Recent experiments such as Super-Kamiokande, SNO, KamLAND, K2K, and MINOS [1, 2, 3, 4, 5, 6], have improved our knowledge of the neutrino mass squared differences (*i.e.*, Δm_{31}^2 and Δm_{21}^2) and some of the leptonic mixing parameters (*i.e.*, θ_{12} , θ_{23}). Whether θ_{13} is different from zero and CP -violation is present in the leptonic sector of the Standard Model are questions which will be addressed by forthcoming experiments [7].

While there exist clear evidence that the $V - A$ structure of the weak interactions of the Standard Model correctly describes neutrino interactions with matter, there is still a possibility that some next-to-leading order mechanism affects the processes of neutrino production and detection. In general, this sort of Physics beyond the Standard Model is described by a set of higher-dimensional non-renormalizable operators suppressed by some high energy scale (see, *e.g.*, Refs. [8, 9] and references therein). The precision measurements in the neutrino sector then open up the possibility to investigate such non-standard interactions (NSI) at a quite accurate level.

Neutrino oscillations and NSI in terrestrial neutrino experiments have been studied extensively in the literature, using the neutrino factory project [10, 11, 12, 13, 14, 15, 16, 17, 18, 19, 20] and other different neutrino facilities (*e.g.*, conventional neutrino beams, super-beams and β -beams) [21, 22, 23, 24, 25, 26, 27] to assess the impact of the NSI in neutrino physics.

Here we adopt a different point of view, we investigate the NSI in the neutrino sector using very high energy neutrinos from astrophysical sources and the capability of neutrino telescopes to measure their fluxes on Earth [28, 29, 30, 31, 32]. We rely on the simplified assumption that the new physics effects arise in the production and detection processes but do not affect the neutrino propagation. We also assume that the lepton mixing matrix is the standard unitary matrix describing the couplings of the charged-lepton–neutrino– W vertices. Moreover, for the sake of illustration, we prefer to study the possible NSI signals for the three different sources (pion, muon damped and neutron sources) separately, as the effects of new physics are quite different in these cases.

This work is organized as follows. In Sec. II, we will present analytic considerations for

the NSI we study in the paper. In particular, we will first describe the detector effects in a unified way, since these are independent of the assumed neutrino source. We will then address the question of non-standard physics in the production processes. In Sec. III, we will describe the statistical approach we use to study the sensitivity of neutrino telescopes to new physics effects and also present our numerical results. Finally, in Sec. IV, we will present a summary of the work as well as our conclusions.

II. NSI AT THE SOURCE AND DETECTOR

We consider NSI through effective four-fermion operators of the form

$$\mathcal{L}_{\text{B-NSI}} = -2\sqrt{2}G_F \cos(\theta_W) \varepsilon_{\alpha\beta}^{ud} [\bar{u}\gamma^\mu P_L d] [\bar{\ell}_\alpha \gamma_\mu P_L \nu_\beta] + \text{h.c.} \quad (1)$$

for charged-current NSI with baryons, where θ_W is the Weinberg angle, and

$$\mathcal{L}_{\ell\text{-NSI}} = -2\sqrt{2}G_F \varepsilon_{\gamma\delta}^{\alpha\beta} [\bar{\ell}_\alpha \gamma^\mu P_L \ell_\beta] [\bar{\nu}_\gamma \gamma_\mu P_L \nu_\delta] \quad (2)$$

for purely leptonic NSI (see [33, 34, 35, 36] for a discussion on the limits on $\varepsilon_{\gamma\delta}^{\alpha\beta}$). While the addition of the hermitian conjugate in the case of NSI with baryons leads to operators of the form $[\bar{d}\gamma^\mu P_L u][\bar{\nu}_\beta \gamma_\mu P_L \ell_\alpha]$, the requirement of a hermitian Lagrangian for the purely leptonic NSI implies $\varepsilon_{\gamma\delta}^{\alpha\beta} = \varepsilon_{\delta\gamma}^{\beta\alpha*}$. In what follows, we will assume that the coherence among the neutrino mass eigenstates that arrive at the Earth has been lost. Thus, we do not need to take any interference terms into account and may treat the source and detector processes separately.

A. Detector effects

Since the detector processes are essentially the same regardless of the source, we will start by considering these. In principle, the detection of astrophysical neutrinos is done through charged-current reactions of the form $\nu + X \rightarrow Y + \ell_\alpha$ and then identifying the neutrino flavor through identification of the outgoing charged lepton. Assuming that the neutrino arrives at the Earth in the mass eigenstate ν_i , the matrix element involved in computing the reaction rate is given by

$$\mathcal{M}_{i\alpha} = \mathcal{M}_0[(1 + \varepsilon^{ud})U]_{\alpha i}, \quad (3)$$

where \mathcal{M}_0 is the matrix element for the corresponding reaction if the incoming neutrino would have been of flavor α and there were no NSI, $\mathbb{1}$ is the 3×3 unit matrix, $\varepsilon^{ud} = (\varepsilon_{\alpha\beta}^{ud})$, and U is the leptonic mixing matrix. Thus, if the incoming ν_i flux is ϕ_i , then the measured flux of ν_α is given by

$$\phi_\alpha = \phi_i |[(\mathbb{1} + \varepsilon^{ud})U]_{\alpha i}|^2. \quad (4)$$

Naturally, the composition of the neutrino flux arriving at the Earth is not purely ν_i . Thus, in order to compute the actual flavor flux, we need to sum over all mass eigenstates and arrive at

$$\phi_\alpha = \sum_i \phi_i |[(\mathbb{1} + \varepsilon^{ud})U]_{\alpha i}|^2. \quad (5)$$

The actual fluxes ϕ_i are dependent on the source type and may also contain effects from the same NSI as those affecting the detector processes.

B. Hadronic sources

Let us first assume that the astrophysical neutrino source creates neutrinos through hadron decays only. Out of the usually considered scenarios, this category includes the muon-damped pion sources (giving initial flavor ratios of $\phi_e : \phi_\mu : \phi_\tau = 0 : 1 : 0$ in the neutrino fluxes) as well as neutron-like sources ($1 : 0 : 0$). These sources produce neutrinos through processes where a meson or baryon decays into a charged lepton of a given flavor¹, a neutrino and possibly other products. When a neutrino is produced together with a charged lepton of flavor β in a weak decay of a meson or a baryon, the probability of producing it in the neutrino mass eigenstate ν_i is given by

$$P_i = |U_{\beta i}|^2 \quad (6)$$

in the Standard Model. With the addition of NSI, there is also the possibility to produce the neutrino in a different flavor state and the corresponding probability changes according to

$$P_i \propto |[(\mathbb{1} + \varepsilon^{ud})U]_{\beta i}|^2. \quad (7)$$

¹ In the case of pion decay, there is a small contamination of decays into electrons which is suppressed by m_e^2/m_μ^2 .

In general, the full expression for P_i also contains a normalization factor, since $\mathbb{1} + \varepsilon^{ud}$ may not be unitary. However, this normalization factor is the same for all P_i and will be removed once we consider neutrino flux ratios. Since the meson/baryon decay gives the only neutrino contribution in this scenario, the ν_i flux will be given by

$$\phi_i = \phi_0 P_i, \quad (8)$$

where ϕ_0 is the total initial neutrino flux. By insertion into Eq. (5), the measured flux of ν_α at the detector is therefore given by

$$\phi_\alpha \propto \phi_0 \sum_i \left| [(\mathbb{1} + \varepsilon^{ud})U]_{\beta i} \right|^2 \left| [(\mathbb{1} + \varepsilon^{ud})U]_{\alpha i} \right|^2. \quad (9)$$

C. Non muon-damped pion sources

We now consider the situation where the source is producing neutrinos both through an initial decay of a charged pion and through the subsequent decay of the resulting charged muon. The complete decay chain is then

$$\begin{array}{ccc} \pi^+ & \longrightarrow & \mu^+ + \nu_\alpha \\ & \downarrow & \\ & e^+ + \nu_\beta + \bar{\nu}_\gamma & \end{array}, \quad (10)$$

as well as the corresponding CP -conjugate reaction for π^- . With only Standard Model interactions, $\alpha = \gamma = \mu$ and $\beta = e$; the produced flavor ratio is then approximately $1 : 2 : 0$.

Mathematically, the decay of the pion can be described in the same way as in the previous section, with the exception that we now need to know the normalization factor for P_i , since we will add the contributions from the pion and muon decays and need to be consistent while doing so. The normalization factor N_μ is simply given by the fact that the total probability of the pion decay should be equal to one, *i.e.*,

$$\sum_i P_i = \frac{1}{N_\mu} \sum_i |[(\mathbb{1} + \varepsilon^{ud})U]_{\mu i}|^2 = 1 \implies N_\mu = [(\mathbb{1} + \varepsilon^{ud})(\mathbb{1} + \varepsilon^{ud\dagger})]_{\mu\mu} \quad (11)$$

(essentially, this is the factor by which the decay rate of the pion would change due to the NSI).

The muon decay is a little more involved, since the final state involves two neutrinos, where one of these is not observed. In the literature, this problem is usually solved by

considering only NSI of the form $[\bar{e}\gamma^\rho P_L\mu][\bar{\nu}_\alpha\gamma_\rho P_L\nu_e]$. With this simplification, the situation is completely analogous to the case of the pion decay, simply because we know the flavor of the outgoing $\bar{\nu}$ (in the case of μ^+ -decay). With general NSI however, we need to consider the full matrix element for the decay $\mu^+ \rightarrow e^+\bar{\nu}_i\nu_j$, which is given by

$$\mathcal{M}_{ij} = \mathcal{M}_0[U^\dagger(\mathcal{J}^{\mu e} + \varepsilon^{\mu e})U]_{ji} \quad (12)$$

where \mathcal{M}_0 is the matrix element when neutrinos do not mix and only Standard Model interactions are considered, $\mathcal{J}_{\alpha\beta}^{\mu e} = \delta_{e\alpha}\delta_{\mu\beta}$, and $\varepsilon^{\mu e} = (\varepsilon_{\alpha\beta}^{\mu e})$ is a matrix containing the strengths of the NSI. In order to obtain the probability for a neutrino from this type of decay to be in the mass eigenstate ν_i , we need to consider the fact that we do not measure the anti-neutrino from the same decay. Thus, the probability will be given by an incoherent sum over the antineutrino mass eigenstates as

$$P_i^{\mu+} \propto \sum_j |\mathcal{M}_{ij}|^2 \propto [U^\dagger(\mathcal{J}^{\mu e} + \varepsilon^{\mu e})^\dagger(\mathcal{J}^{\mu e} + \varepsilon^{\mu e})U]_{ii}. \quad (13)$$

Again, this needs to be normalized and the normalization factor is given by

$$N^{\mu+} = \text{Tr}[(\mathcal{J}^{\mu e} + \varepsilon^{\mu e})^\dagger(\mathcal{J}^{\mu e} + \varepsilon^{\mu e})] \quad (14)$$

The corresponding argumentation for the outgoing antineutrino results in

$$\bar{P}_j^{\mu+} \propto \sum_i |\mathcal{M}_{ij}|^2 \propto [U^\dagger(\mathcal{J}^{\mu e} + \varepsilon^{\mu e})(\mathcal{J}^{\mu e} + \varepsilon^{\mu e})^\dagger U]_{jj} \quad (15)$$

with the same normalization constant $\bar{N}^{\mu+} = N^{\mu+}$. Repeating the same derivation for μ^- -decay, we arrive at $P_i^{\mu-} = \bar{P}_i^{\mu+}$ and $\bar{P}_j^{\mu-} = P_j^{\mu+}$. Thus, assuming equal numbers of positive and negative pions decaying, the flux of neutrino mass eigenstate ν_i (or antineutrino mass eigenstate $\bar{\nu}_i$) is given by

$$\phi_i = \phi_0(P_i + P_i^{\mu+} + \bar{P}_i^{\mu+}), \quad (16)$$

where ϕ_0 is the initial flux of ν_e in the case of Standard Model interactions only.

III. EXPERIMENTAL IMPLICATIONS

For experimental reasons, it is customary to consider the flavor flux ratios

$$R_{e\mu} = \frac{\phi_e}{\phi_\mu}, \quad R_{\mu\tau} = \frac{\phi_\mu}{\phi_\tau}, \quad \text{and} \quad R = \frac{\phi_\mu}{\phi_e + \phi_\tau} \quad (17)$$

(note that these are not independent). With the flavor fluxes computed as in Sec. II, we want to know how NSI at the source and detector can affect the results of these measurements. In order to do this, we will examine how well a measured value of any of the R s can be accommodated when considering Standard Model interactions only, as well as when allowing for NSI. To quantify this, we introduce the χ^2 function

$$\chi^2(x) = \sum_i \left(\frac{R_i^{\text{exp}} - R_i^{\text{th}}(x)}{\sigma_{R_i}} \right)^2 + \sum_j \left(\frac{x_j - x_{j,0}}{\sigma_{x_j}} \right)^2. \quad (18)$$

Here, R_i^{exp} is the measured value of a given ratio, $R_i^{\text{th}}(x)$ is the theoretically expected value computed from the set x of input parameters, σ_{R_i} is the experimental uncertainty in R_i , i is an index running over the flux ratios considered, σ_{x_j} are the external uncertainties for the input parameters, and j is an index running over the input parameters. In the case of Standard Model interactions only, x contains the neutrino mixing parameters, while in the NSI scenario it also contains all of the different ε s. How well a particular measured combination of R^{exp} s can be accommodated within a model is then quantified by

$$\chi_{\min}^2 = \min_x [\chi^2(x)], \quad (19)$$

which is χ^2 distributed with n degrees of freedom, where n is the number of independent flavor flux ratios considered.

In the following numerical computations, we adopt the standard parametrization of the neutrino mixing matrix (see Refs. [37, 38, 39, 40, 41]), assuming also a tri-bimaximal structure [42] for it. We assume the 3σ errors on the standard mixing parameters to be of the same order as the errors in Ref. [43]. In Tab. I, we give the corresponding values for these parameters.

A. Muon-damped pion sources

In order to appreciate the effects of the new physics on the flux ratios of Eq. (17), it is useful to recall the Standard Model expectations for these quantities. Putting $\varepsilon^{ud} = 0$ and

<i>Parameter</i>	<i>Best fit</i>	<i>3σ error</i>
θ_{12}	35.3°	5°
θ_{13}	0	12.5°
θ_{23}	45°	10°
δ	Free ($[0, 2\pi]$)	

TABLE I: *Summary of the best fit values and 3σ errors used in our numerical computation for the standard neutrino oscillation parameters.*

$\beta = \mu$ in Eq. (9), we get the following expressions for the flavor fluxes:

$$\begin{aligned}
\phi_e &= \phi_0 \sum_i |U_{\mu i}|^2 |U_{ei}|^2, \\
\phi_\mu &= \phi_0 \sum_i |U_{\mu i}|^4, \\
\phi_\tau &= \phi_0 \sum_i |U_{\mu i}|^2 |U_{\tau i}|^2.
\end{aligned} \tag{20}$$

In the limit of exact tri-bimaximal mixing ($\theta_{13} = 0$, $\sin^2 \theta_{12} = 1/3$, and $\sin^2 \theta_{23} = 1/2$ [42]), we obtain:

$$R_{e\mu} = \frac{4}{7}, \quad R_{\mu\tau} = 1, \quad \text{and} \quad R = \frac{7}{11}. \tag{21}$$

Before concluding that large deviations from these values are signals of new physics, we should carefully take the role of the uncertainties of the standard parameters into account [44]. In order to do that, we compute the distributions of the three ratios, extracting neutrino mixing angles according to Gaussian distributions with central values and 1σ error as deducible from Tab. I. The result of this procedure is shown in Fig. 1. It can be clearly seen that the larger spread is obtained for $R_{e\mu}$, due to the uncertainties on the mixing angles θ_{12} , θ_{23} and on the product $\cos \delta \theta_{13}$ (see also Eq. (4) in Ref. [45]), which are all of the same order of magnitude. On the other hand, the fact that most decays will result in neutrinos of the mass eigenstate with the largest ν_μ content protects $R_{\mu\tau}$ from becoming much smaller than one, an effect that can also be seen in the ratio R , which cannot be much smaller than $1/2$. The pile-up of the distributions close to these values are the results of θ_{23} being close to maximal. It is then possible that new physics effects would be much more visible in the ratios containing τ neutrinos and, for this reason, we will investigate the effects of the ε parameters in the $R_{\mu\tau}$ - R -plane.

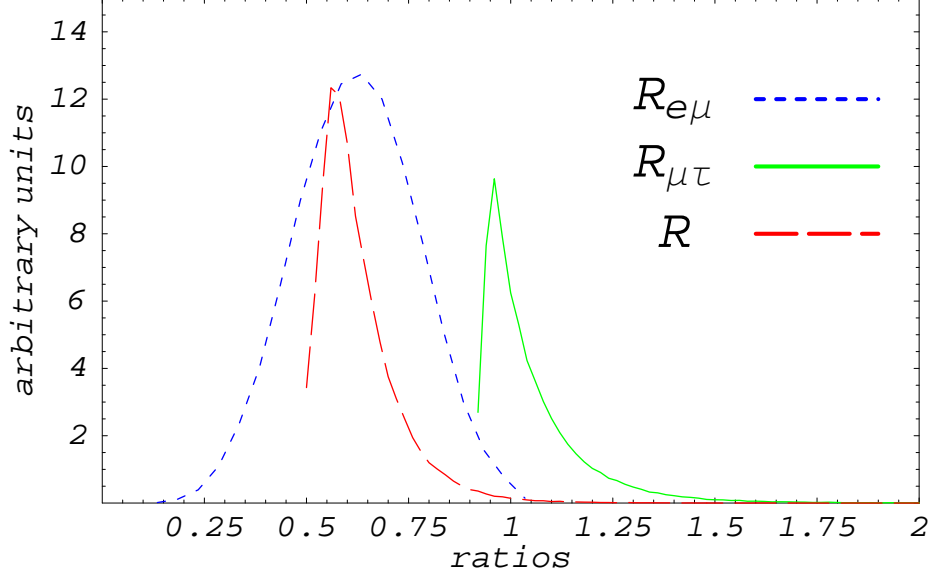


FIG. 1: Statistical distribution (in arbitrary units) of the flux ratios $R_{e\mu}$ (dashed line), $R_{\mu\tau}$ (solid line) and R (long-dashed line), as computed in the Standard Model for a muon-damped pion source.

The correlation between $R_{\mu\tau}$ and R can be analyzed using the χ^2 definition in Eq. (18). A crucial point here is the precision we expect in the experimental measurement of the flux ratios, σ_{R_i} ; for the sake of illustration, we will assume that $\sigma_{R_i} = 0.1R_i^{\text{exp}}$ for any ratio (the effect of changing this value is discussed in Sec. III E), which means that they are measured with a 10 % error. In addition, we assume an external error of 0.1 for the ε parameters. The reason for choosing such a large error is that we are mainly interested in the qualitative impact of the parameters rather than making precise predictions. The results of the minimization of the χ^2 over all model parameters is shown in Fig. 2. We note that the extension of the isocontours produced by new physics is predominantly in the direction of large ratios; in particular, $R_{\mu\tau}$ and R can be as large as twice their tri-bimaximal mixing values, thus an experimental signal in this direction could be ascribed to the effects of non-standard interaction type described in this paper. The extension of the contours to small values of the flavor flux ratios (*e.g.*, $R_{\mu\tau} \sim 0.5$, to be compared with Fig. 1) even in the standard case can be attributed to the finite resolution assumed for the measurements.

It is interesting to understand which of the new parameters that cause the largest deviations from the Standard Model prediction. This is illustrated in Fig. 3, where we show the isocontours of χ_{min}^2 in the $R_{\mu\tau}$ - R -plane when allowing for only one non-zero ε at a time.

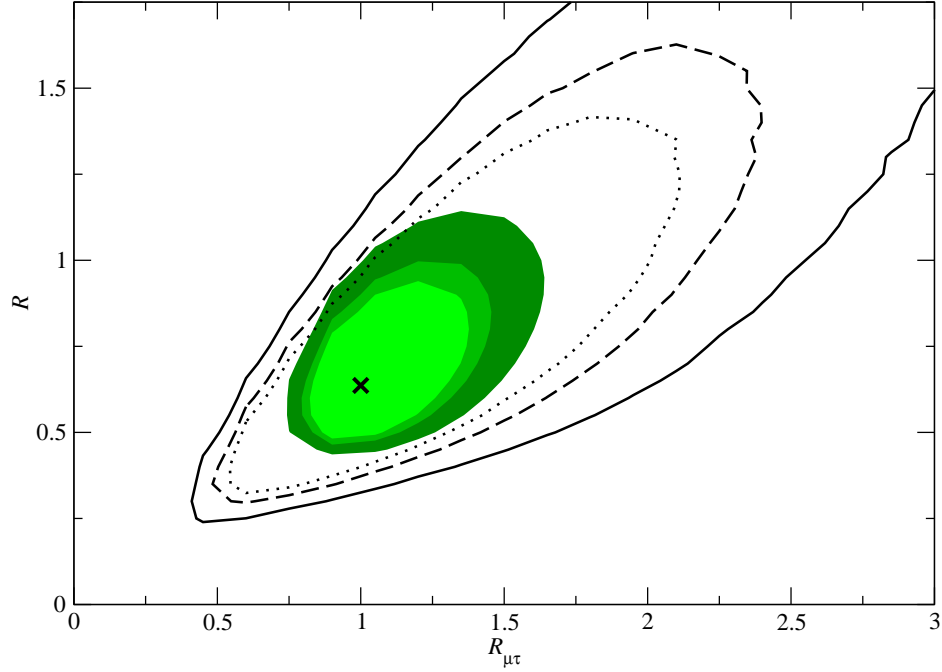


FIG. 2: Isocontours of χ^2_{\min} in the $R_{\mu\tau}$ – R -plane in the case of a muon damped pion source in the standard framework for neutrino oscillation and interaction (shaded regions) as well as for the framework with included NSI (black curves). The contours correspond to 90 %, 95 %, and 99 % C.L., respectively. The black cross corresponds to the prediction in the case of tribimaximal mixing in the standard framework.

From this figure, it is clear that the most relevant contributions to the extension come from $\varepsilon_{\mu\mu}^{ud}, \varepsilon_{\mu\tau}^{ud}$ and $\varepsilon_{\tau\tau}^{ud}$. Thus, these are the parameters to which neutrino telescopes would be most sensitive. Putting stringent bounds on these parameters would therefore be useful for making more robust predictions for the flavor flux ratios in the case of the muon-damped pion source. Note that none of the outer contours from varying individual ε reach the 99 % C.L. contour from the full simulation. This implies that in order to accommodate these contours in the full simulation, some combination of different ε s is needed.

B. Neutron-like sources

In the case when the source of the astrophysical neutrino flux is neutron-like (*i.e.*, essentially a beta decay), then the considerations corresponding to those made for the muon-

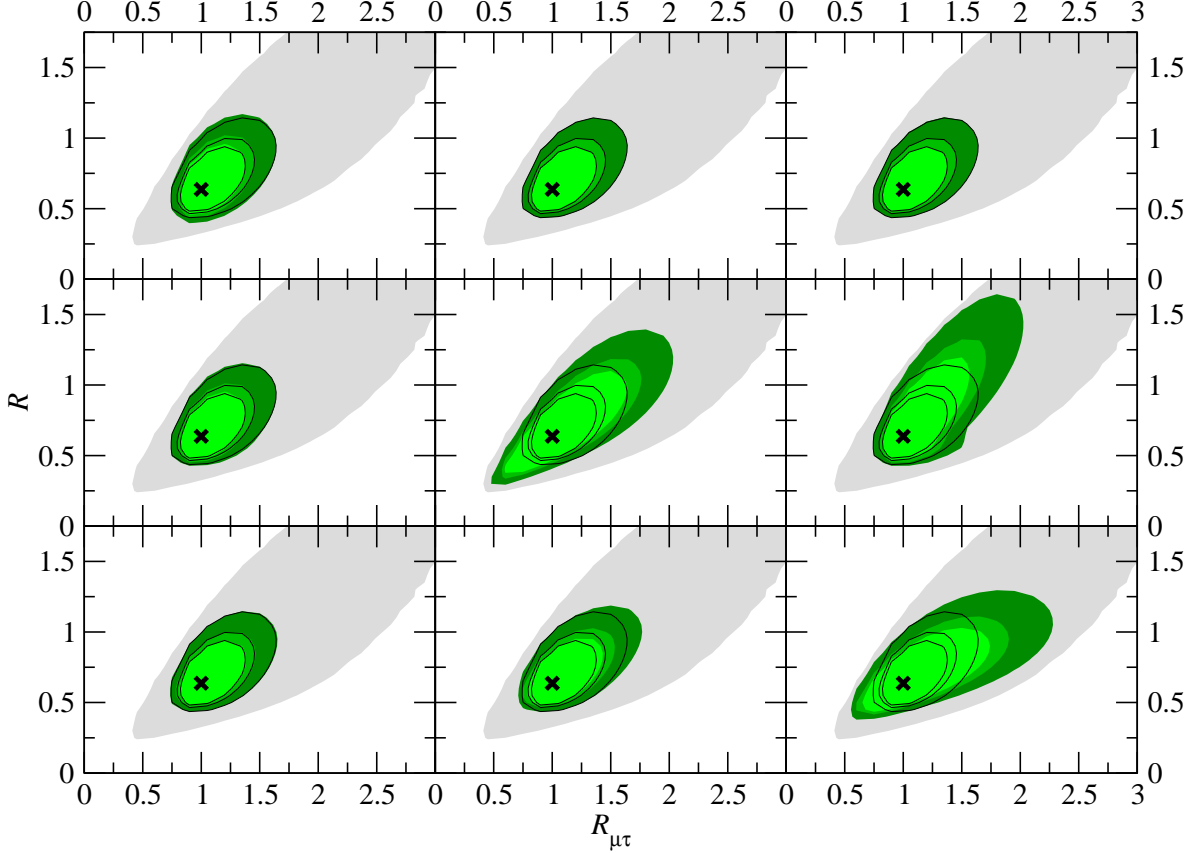


FIG. 3: Isocontours of χ^2_{\min} in the $R_{\mu\tau}$ – R -plane in the case of a muon-damped pion source. The black curves correspond to the case with only Standard Model interactions, while the three inner shaded regions are produced allowing one ε to vary with an external input error of 0.1 at 1σ . The panels are placed such that the ε varied has the same position in the ε^{ud} matrix as the plot has in the figure, i.e., the upper right plot corresponds to allowing $\varepsilon_{e\tau}^{ud}$ to vary (we put the neutrino flavors in the order $\{\nu_e, \nu_\mu, \nu_\tau\}$). The contours correspond to 90 %, 95 %, and 99 % C.L., respectively. The outer shaded region is the 99 % C.L. contour from the full NSI simulation. The black crosses correspond to the prediction from tribimaximal mixing in the standard framework.

damped pion sources result in the flavor flux ratios

$$R_{e\mu} = \frac{5}{2}, \quad R_{\mu\tau} = 1, \quad \text{and} \quad R = \frac{2}{7}, \quad (22)$$

in the case of tribimaximal mixing. Figure 4 shows the isocontours of χ^2_{\min} in the $R_{\mu\tau}$ – R -plane for a neutron-like source using the same procedure as that described in the previous section. In this case, the extension of the isocontours is mainly in the direction of increasing

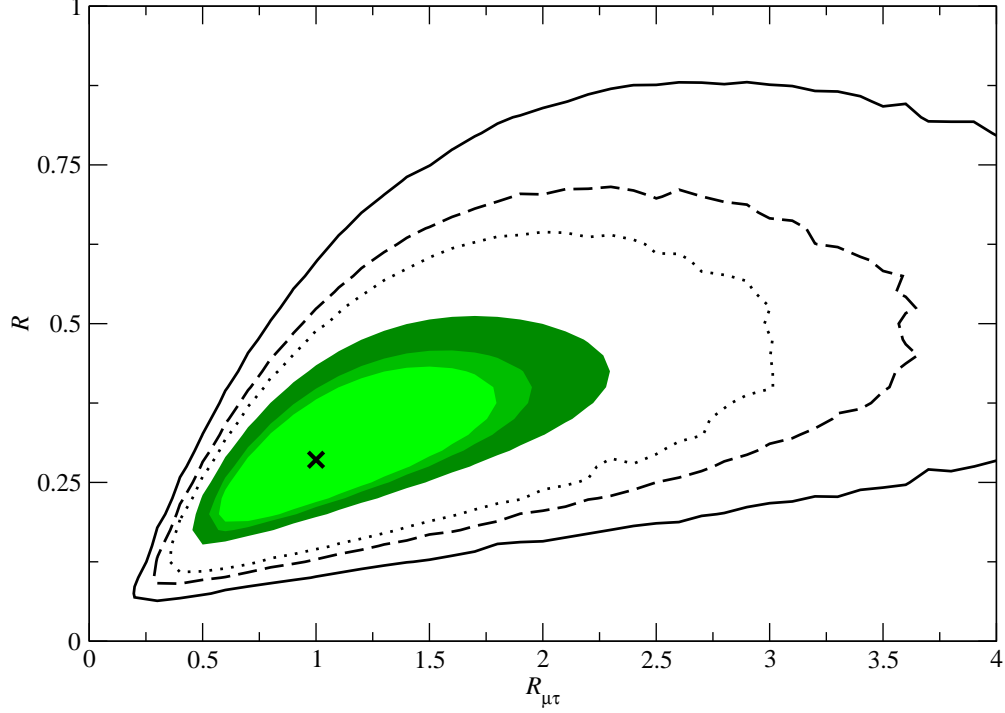


FIG. 4: Isocontours of χ^2_{\min} in the $R_{\mu\tau}$ – R -plane in the case of a neutron-like source in the standard framework for neutrino oscillation and interaction (shaded regions) as well as for the framework with included NSI (black curves). The contours correspond to 90 %, 95 %, and 99 % C.L., respectively. The black cross corresponds to the prediction in the case of tribimaximal mixing in the standard framework.

$R_{\mu\tau}$, corresponding in an increase in the ν_e flux on the expense of ν_τ compared to the standard setup. However, this extension more or less has the same shape as the extension in the standard case and the big errors for large values of the flavor flux ratios can be somewhat attributed to the increasing absolute errors on σ_{R_i} .

In Fig. 5, we show the impacts of the individual ε parameters for a neutron-like source. Unlike the case of the muon-damped pion source, with a neutron-like source we find that all of the ε has at least some small impact on the flavor flux ratios, even if it is still relatively small. The largest difference is observed for the $\varepsilon_{\tau\mu}^{ud}$ parameter, which (together with $\varepsilon_{\tau\tau}^{ud}$) seems to be the source of the extension to larger $R_{\mu\tau}$ with R being essentially constant. Also the impact of ε_{ee}^{ud} is peculiar, even if it is not as large as that of $\varepsilon_{\tau\mu}^{ud}$. It would seem that this parameter fixes $R_{\mu\tau}$ while altering R , signifying a change in the flux of ν_e compared to the

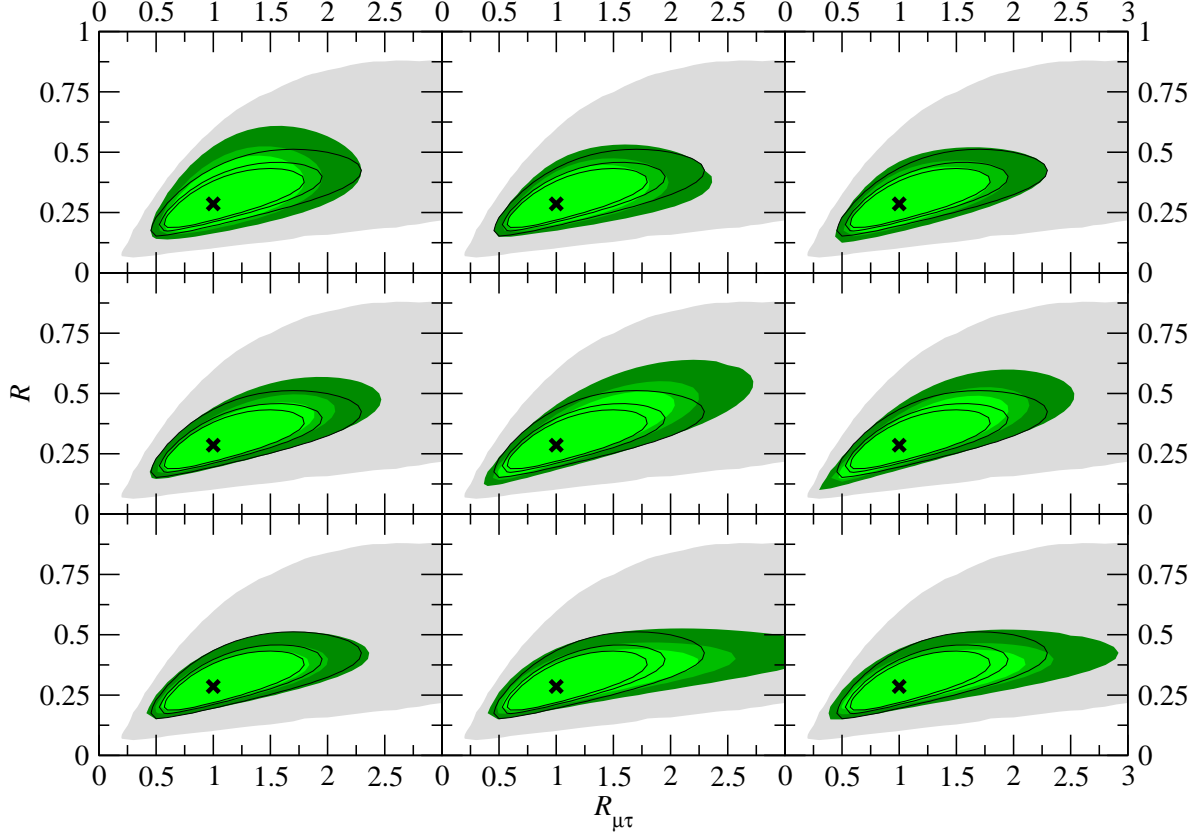


FIG. 5: Isocontours of χ^2_{\min} in the $R_{\mu\tau}$ - R -plane in the case of a neutron-like source. The black curves correspond to the case with only Standard Model interactions, while the three inner shaded regions are produced allowing one ε to vary with an external input error of 0.1 at 1σ . The panels are placed such that the ε varied has the same position in the ε^{ud} matrix as the plot has in the figure, i.e., the upper right plot corresponds to allowing $\varepsilon^{ud}_{e\tau}$ to vary (we put the neutrino flavors in the order $\{\nu_e, \nu_\mu, \nu_\tau\}$). The contours correspond to 90 %, 95 %, and 99 % C.L., respectively. The outer shaded region is the 99 % C.L. contour from the full NSI simulation. The black crosses correspond to the prediction from tribimaximal mixing in the standard framework.

other two species.

C. Non muon-damped pion sources

As discussed in Sec. II, when a pion source is not muon-damped, there will essentially be two different sources of neutrinos – the pion decay and the subsequent decay of the muon.

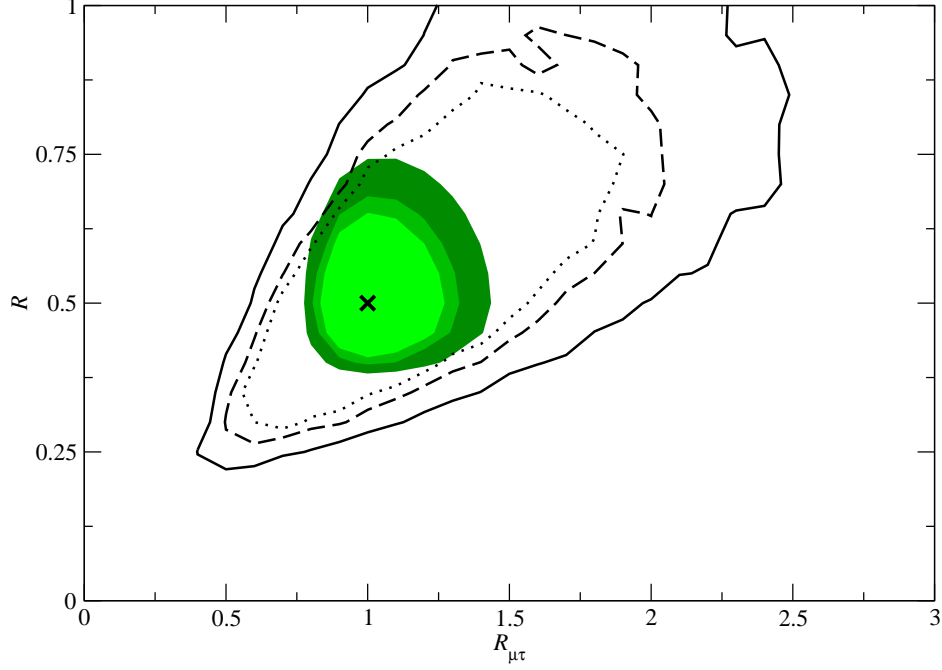


FIG. 6: Isocontours of χ^2_{\min} in the $R_{\mu\tau}$ - R -plane in the case of a non muon-damped pion source in the standard framework for neutrino oscillation and interaction (shaded regions) as well as for the framework with included NSI (black curves). The contours correspond to 90 %, 95 %, and 99 % C.L., respectively. The black cross corresponds to the prediction in the case of tribimaximal mixing in the standard framework.

Since the NSI involved in the two different processes do not depend upon the same ε s, the effective parameter space is increased quite dramatically, even compared to the previously considered NSI scenarios. For this type of source, the prediction of tribimaximal lepton mixing is given by

$$R_{e\mu} = 1, \quad R_{\mu\tau} = 1, \quad \text{and} \quad R = \frac{1}{2}, \quad (23)$$

simply due to the fact that the flavor fluxes are predicted to be equal.

In Fig. 6, we show the results of the minimization of χ^2 both for the standard case and when allowing for NSI (both in the pion and muon decays). For large values of $R_{\mu\tau}$ and R in the NSI case, this figure is not very smooth. The reason for this is that the χ^2 is now a function of a very large number of parameters and the minimization procedure is not always able to find the actual minimum. In this scenario, we see that the extension of the contours due to NSI is mainly along the direction of constant $R/R_{\mu\tau}$, corresponding to a fixed ratio

between the ν_e and ν_τ fluxes while the relative ν_μ flux varies (again, the smaller size of the regions for smaller R_i is mainly due to the differences in σ_{R_i}).

As in the previous scenarios, we present the dependence on individual ε s in Fig. 7. Here, the exception is that the parameter space now consists of an additional nine ε s, which we illustrate by two different plots for the dependencies on the ε^{ud} and $\varepsilon^{\mu e}$, respectively.

The effects of the ε^{ud} parameters are very similar to what they were in the case of the muon-damped pion source, although a bit less pronounced. This is to be expected, since the processes of the muon-damped source also play a role in the case when the muons are not damped – although the effect is less pronounced as there are also other processes involved. However, the effects of the $\varepsilon^{\mu e}$ parameters are essentially negligible, with the only parameter actually showing any difference (although still a very small one) being $\varepsilon_{e\tau}^{\mu e}$. Thus, it would seem that the $\varepsilon^{\mu e}$ cannot play a significant role when it comes to astrophysical neutrino fluxes.

D. Comparison of scenarios

An important aspect in the study of astrophysical neutrino fluxes is what we could learn about the source from studying the flavor composition of the flux (*i.e.*, what type of source that is providing the flux). Thus, in Fig. 8, we show the 99 % C.L. contours for all of the source types discussed above. As can be seen in this figure, the pion sources could be relatively well separated from the neutron-like sources in the standard scenario, while it could be harder to tell whether there is muon-damping or not in a pion source. This conclusion is not significantly altered when taking NSI into account, although it will be a little harder to tell the sources apart if flavor ratios in the region expected from Standard Model interactions only are measured. However, since the NSI mainly extend the contours in different directions for different scenarios, large parts of the space of possible measurements allowed in the case of a neutron-like source are not allowed for pion sources and vice versa. Still, telling if there is muon-damping in a pion source remains a difficult endeavour. The contour extension due the NSI also has another intriguing property. Since the extensions are mainly not in the direction to where other scenarios are located, there is a fair chance that if NSI actually appear in the flavor flux ratios, their effect could not be misinterpreted as simply being due to a different neutrino source.

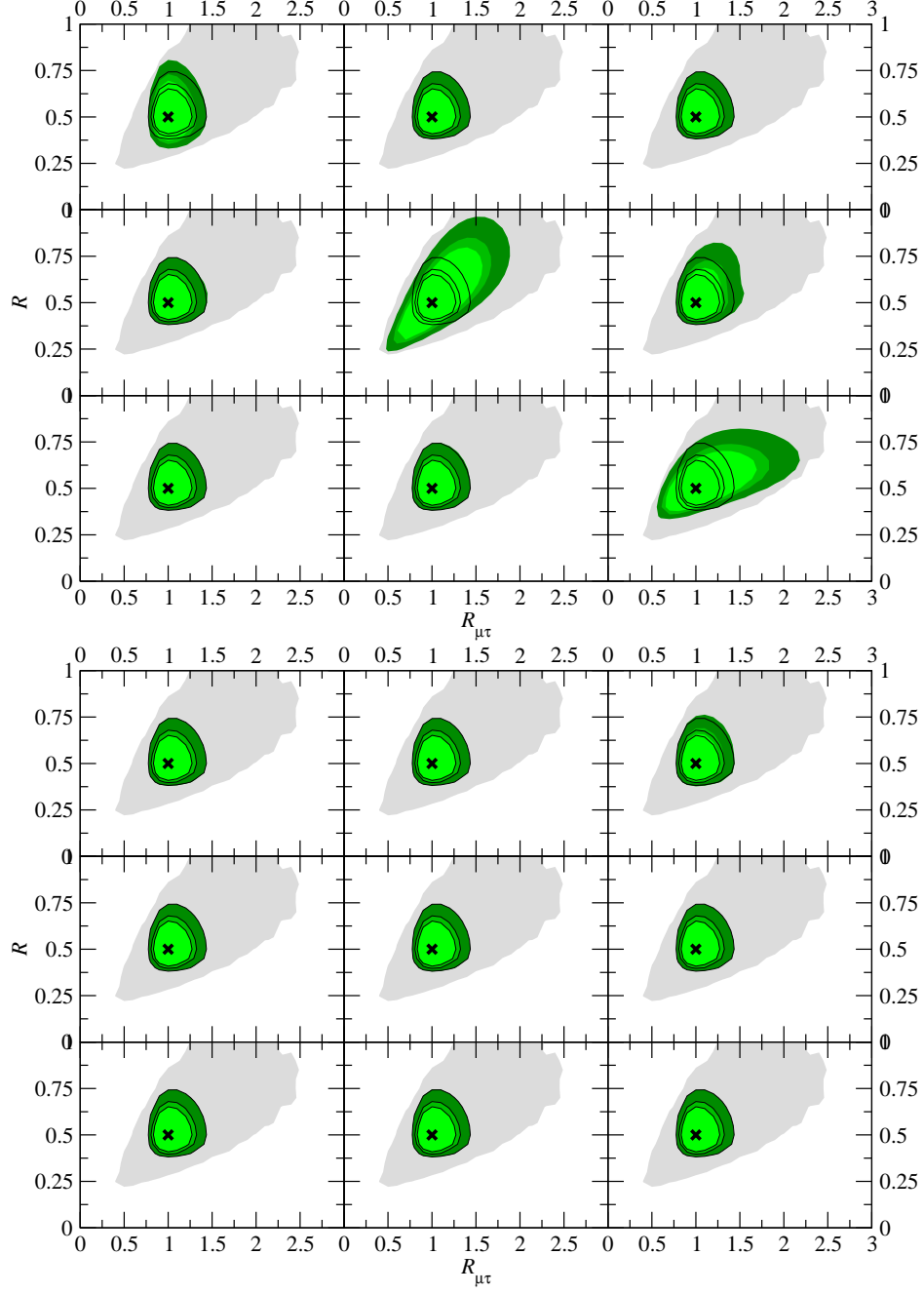


FIG. 7: Isocontours of χ^2_{\min} in the $R_{\mu\tau}$ – R -plane in the case of a non muon-damped pion source. The black curves correspond to the case with only Standard Model interactions, while the three inner shaded regions are produced allowing one ϵ to vary with an external input error of 0.1 at 1σ . The upper plot shows the dependence on the ϵ^{ud} and the lower plot the dependence on the $\epsilon^{\mu e}$. The panels are placed such that the ϵ varied has the same position in the matrices as the plot has in the figure, i.e., the upper right panel of the upper plot corresponds to allowing $\epsilon_{e\tau}^{ud}$ to vary. The elements of the figure are the same as in the previous plots.

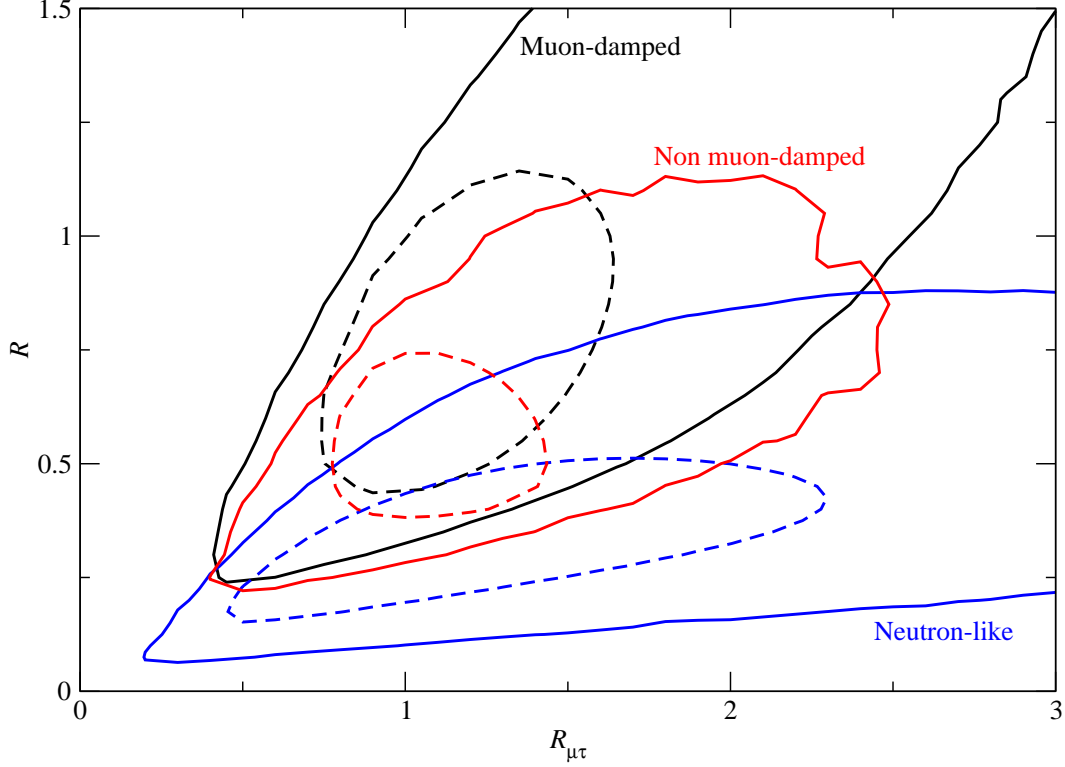


FIG. 8: The 99 % C.L. isocontours in the $R_{\mu\tau}$ - R -plane for the sources we have discussed. The solid lines correspond to the contours when allowing for general NSI, while the dashed contours correspond to the result in the case of Standard Model interactions only.

E. Impact of experimental uncertainties

As mentioned earlier, the experimental precision with which the neutrino flavor flux ratios can be measured is an important part of our analysis. In our discussions so far, we have assumed a relative error of 10 % and it is of importance to understand how this affects our results. For this purpose, Fig. 9 shows the full result for the muon-damped source both with our initial assumption of $\sigma_{R_i} = 0.1R_i^{\text{exp}}$ as well as with a more optimistic assumption of $\sigma_{R_i} = 0.05R_i^{\text{exp}}$. As can be seen in this figure, a better experimental resolution makes the NSI degeneracies more pronounced. This is to be expected, since better measurements allow for better opportunities to extract information of the underlying physics. Conversely, if the resolution is made worse, it will become harder to distinguish the NSI degeneracies from the standard scenario as deviations could simply be due to experimental uncertainties.

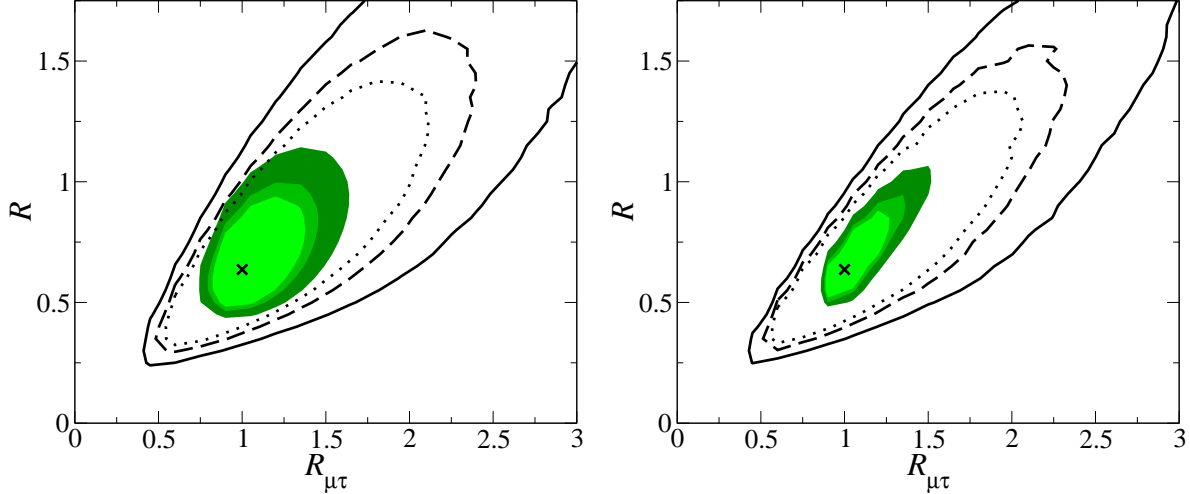


FIG. 9: The isocontours in the $R_{\mu\tau}$ - R -plane in the case of a muon-damped source assuming different experimental resolutions for the flavor flux ratios. The left panel assumes $\sigma_{R_i} = 0.1 R_i^{\text{exp}}$ (i.e., identical to Fig. 2), while the right panel assumes $\sigma_{R_i} = 0.05 R_i^{\text{exp}}$. The elements of the plots are the same as in Fig. 2.

IV. SUMMARY AND CONCLUSIONS

In this paper we analyzed the impact of new physics effects in the production and detection of astrophysical neutrinos. Detection processes were considered independent of the source producing neutrinos and the possible new physics effects were parametrized in terms of the matrix $\varepsilon_{\alpha\beta}^{ud}$ which alters the charged-current reaction $\nu + X \rightarrow Y + \ell_\alpha$ involving leptons and hadrons. The same matrix also intervenes in the production of neutrinos from muon-damped pion sources (in which neutrinos coming from subsequent muon decays do not contribute to the measurable neutrino flux on Earth) and from neutron-like sources. If muon decays also play a role in the production of neutrinos (as in the case of the “standard” pion sources), then a new set of parameters $\varepsilon_{\alpha\beta}^{\mu e}$ should be introduced to take the purely leptonic process into account. Since the fluxes of astrophysical neutrinos can be measured at neutrino telescopes, we have considered the experimentally accessible flux ratios $R_{\mu\tau} = \phi_\mu/\phi_\tau$ and $R = \phi_\mu/(\phi_e + \phi_\tau)$, in order to investigate the effects of the new parameters. This was done through a χ^2 analysis to see how well the neutrino flux ratios at neutrino telescopes can be accommodated in different models, assuming tri-bimaximal mixing as an external central value for the standard neutrino oscillation parameters. Making this analysis in the Stan-

Standard Model first and then including the NSI gave us insight of how new physics can affect the possible ranges of these observables. Our results can be summarized in the simplified scenario, where only one source at a time is responsible for the neutrino flux on Earth. In particular, for muon-damped sources, we found that with NSI, the measured flux ratios can be significantly larger than their tri-bimaximal mixing values, an effect mainly due to $\varepsilon_{\mu\mu}^{ud}$, $\varepsilon_{\mu\tau}^{ud}$ and $\varepsilon_{\tau\tau}^{ud}$. Also for neutron-like sources the extension of the contour plots obtained including NSI effects are in the direction of increasing $R_{\mu\tau}$, with R being essentially constant (thus a significant change in the ν_e flux is at work). Moreover, all the epsilon parameters contribute, in some extent, to the shift of the flavor flux ratios. The analysis of the non muon-damped sources is more complicated. This is due to the two independent classes of new parameters entering in the game. However, while both R and $R_{\mu\tau}$ can be sizably different from the Standard Model predictions, we found that the leptonic $\varepsilon_{\alpha\beta}^{\mu e}$ have negligible impacts on these results. In principle it is possible, in both Standard Model and new physics scenarios, to learn something about the source, since the observational parameter space covered by the flux ratios from one particular source does not overlap significantly with that of another source.

It should be noted that all of our considerations depend on the assumed uncertainties on the extraction of the flux ratios as well as on how well the standard neutrino oscillation parameters have been determined. In fact, although smaller σ_{R_i} makes the NSI effects more pronounced, larger σ_{R_i} will completely overshadow any significant new physics effect. In addition, we have considered relatively large values of the NSI parameters. It should therefore also be noted that the effect of small NSI will become increasingly difficult to observe unless the flavor flux ratios and standard neutrino oscillation parameters can be very accurately determined.

Acknowledgments

The authors would like to thank Tommy Ohlsson and He Zhang for reading the manuscript and providing useful comments.

This work was supported by the Swedish Research Council (Vetenskapsrådet), contract no. 623-2007-8066 [M.B.]. This work has been partly supported by the Italian Ministero dell

- [1] J. Hosaka et al. (Super-Kamiokande), Phys. Rev. **D74**, 032002 (2006), hep-ex/0604011.
- [2] S. N. Ahmed et al. (SNO), Phys. Rev. Lett. **92**, 181301 (2004), nucl-ex/0309004.
- [3] N. Oblath (SNO), AIP Conf. Proc. **947**, 249 (2007).
- [4] M. H. Ahn et al. (K2K), Phys. Rev. **D74**, 072003 (2006), hep-ex/0606032.
- [5] D. G. Michael et al. (MINOS), Phys. Rev. Lett. **97**, 191801 (2006), hep-ex/0607088.
- [6] S. Abe et al. (KamLAND) (2008), 0801.4589.
- [7] A. Bandyopadhyay et al. (ISS Physics Working Group) (2007), 0710.4947.
- [8] M. B. Gavela, D. Hernandez, T. Ota, and W. Winter (2008), 0809.3451.
- [9] S. Antusch, J. P. Baumann, and E. Fernandez-Martinez (2008), 0807.1003.
- [10] P. Huber, T. Schwetz, and J. W. F. Valle, Phys. Rev. **D66**, 013006 (2002), hep-ph/0202048.
- [11] T. Ota, J. Sato, and N.-a. Yamashita, Phys. Rev. **D65**, 093015 (2002), hep-ph/0112329.
- [12] M. C. Gonzalez-Garcia, Y. Grossman, A. Gusso, and Y. Nir, Phys. Rev. **D64**, 096006 (2001), hep-ph/0105159.
- [13] A. M. Gago, M. M. Guzzo, H. Nunokawa, W. J. C. Teves, and R. Zukanovich-Funchal, Phys. Rev. **D64**, 073003 (2001), hep-ph/0105196.
- [14] P. Huber and J. W. F. Valle, Phys. Lett. **B523**, 151 (2001), hep-ph/0108193.
- [15] J. Kopp, M. Lindner, and T. Ota, Phys. Rev. **D76**, 013001 (2007), hep-ph/0702269.
- [16] N. C. Ribeiro, H. Minakata, H. Nunokawa, S. Uchinami, and R. Zukanovich-Funchal, JHEP **12**, 002 (2007), 0709.1980.
- [17] J. Kopp, T. Ota, and W. Winter, Phys. Rev. **D78**, 053007 (2008), 0804.2261.
- [18] W. Winter (2008), 0808.3583.
- [19] G. Altarelli and D. Meloni (2008), 0809.1041.
- [20] M. Campanelli and A. Romanino, Phys. Rev. **D66**, 113001 (2002), hep-ph/0207350.
- [21] M. Honda, N. Okamura, and T. Takeuchi (2006), hep-ph/0603268.
- [22] R. Adhikari, S. K. Agarwalla, and A. Raychaudhuri, Phys. Lett. **B642**, 111 (2006), hep-ph/0608034.
- [23] M. Blennow, T. Ohlsson, and J. Skrotzki, Phys. Lett. **B660**, 522 (2008), arXiv.org:hep-ph/0702059.

- [24] J. Kopp, M. Lindner, T. Ota, and J. Sato, Phys. Rev. **D77**, 013007 (2008), 0708.0152.
- [25] N. Kitazawa, H. Sugiyama, and O. Yasuda (2006), hep-ph/0606013.
- [26] M. Blennow, D. Meloni, T. Ohlsson, F. Terranova, and M. Westerberg, Eur. Phys. J. **C56**, 529 (2008), 0804.2744.
- [27] T. Ohlsson and H. Zhang (2008), 0809.4835.
- [28] IceCube collaboration homepage, <http://icecube.wisc.edu/>.
- [29] Baikal collaboration homepage, <http://www.ifh.de/baikal/baikalhome.html>.
- [30] ANTARES collaboration homepage, <http://antares.in2p3.fr/index.html>.
- [31] NESTOR collaboration homepage, <http://www.nestor.org.gr/>.
- [32] NEMO collaboration homepage, <http://nemoweb.lns.infn.it/project.htm>.
- [33] J. Barranco, O. G. Miranda, C. A. Moura, and J. W. F. Valle, Phys. Rev. **D77**, 093014 (2008), 0711.0698.
- [34] S. Davidson, C. Pena-Garay, N. Rius, and A. Santamaria, JHEP **03**, 011 (2003), hep-ph/0302093.
- [35] Z. Berezhiani and A. Rossi, Phys. Lett. **B535**, 207 (2002), hep-ph/0111137.
- [36] J. Barranco, O. G. Miranda, C. A. Moura, and J. W. F. Valle, Phys. Rev. **D73**, 113001 (2006), hep-ph/0512195.
- [37] B. Pontecorvo, Sov. Phys. JETP **6**, 429 (1957).
- [38] Z. Maki, M. Nakagawa, and S. Sakata, Prog. Theor. Phys. **28**, 870 (1962).
- [39] B. Pontecorvo, Sov. Phys. JETP **26**, 984 (1968).
- [40] V. N. Gribov and B. Pontecorvo, Phys. Lett. **B28**, 493 (1969).
- [41] L.-L. Chau and W.-Y. Keung, Phys. Rev. Lett. **53**, 1802 (1984).
- [42] P. F. Harrison, D. H. Perkins, and W. G. Scott, Phys. Lett. **B530**, 167 (2002).
- [43] M. Maltoni, T. Schwetz, M. A. Tortola, and J. W. F. Valle, New J. Phys. **6**, 122 (2004), preprint updated after publication, hep-ph/0405172v6.
- [44] D. Meloni and T. Ohlsson, Phys. Rev. **D75**, 125017 (2007).
- [45] P. Lipari, M. Lusignoli, and D. Meloni, Phys. Rev. **D75**, 123005 (2007), 0704.0718.